Evaluating the structural performance of masonry walls incorporating recycled plastic bricks under monotonic and cyclic loading

Youcef Moulai Arbi[a], *Noureddine* Mahmoudi[b], *Mohammed* Bentahar[c]

[a] University of Mustapha Stambouli, Laboratory of Quantum Physics of Matter and Mathematical Modeling (LPQ3M), Mascara, People's Democratic Republic of Algeria, e-mail: youcef.moulaiarbi@univ-mascara.dz, **corresponding author**, ORCID ID: https://orcid.org/0000-0002-6534-8820

[b] Universiy of Saida Dr. Moulay Tahar, Faculty of Technology, Department of Civil Engineering and Hydraulics, Saida, People's Democratic Republic of Algeria, e-mail: mahmoudi.noureddine@yahoo.fr, ORCID ID: https://orcid.org/0000-0002-9740-0857

[c] Universiy of Saida Dr. Moulay Tahar, Faculty of Technology, Department of Civil Engineering and Hydraulics, Saida, People's Democratic Republic of Algeria, e-mail: bentahae@yahoo.fr, ORCID ID: https://orcid.org/0000-0002-2166-678X

https://doi.org/10.5937/vojtehg72-50560

FIELD: mechanical engineering, civil engineering
ARTICLE TYPE: original scientific paper

Abstract:

Introduction/purpose:This study evaluates the structural performance of masonry walls made from recycled plastic bricks under monotonic and cyclic loading. The purpose was to investigate the feasibility of using recycled plastic bricks as an alternative for masonry construction, focusing on their structural viability and potential environmental benefits.

Methods:A simplified micro-modeling approach in Abaqus was employed to simulate the behavior of these walls. The plastic bricks were represented with solid elements, while the mortar joints were modeled through cohesive interactions. The numerical model underwent validation through a mesh sensitivity analysis and was subjected to vertical compression followed by horizontal loading.

Results:The findings indicated a reduction in strength compared to traditional masonry materials. However, the study successfully captured the structural response and damage evolution of masonry walls under the specified loading conditions. Despite the reduced strength, the structural

viability of recycled plastic bricks was strongly affirmed, and the behavior observed under load conditions was particularly informative.

Conclusions:The investigation underscored the potential of plastic composite bricks in contributing to sustainable building practices. The outcomes validated the feasibility of incorporating plastic bricks into construction, highlighting their environmental benefits and sustainable implications. This study advanced the field of sustainable construction materials by demonstrating the practical application and benefits of using recycled plastic bricks.

Key words: finite element analysis, plastic bricks, masonry wall, in-plane loads, in-plan cyclic loads.

Introduction

Masonry is one of the oldest and most used building materials throughout the world because of its rich history spreading over hundreds of years. It has been used widely among various cultures and regions of the world in construction. Masonry is made up of filled units, like bricks, stones, or blocks, with mortar. These units, in their turn, can consist of different materials and possess some mechanical characteristics (Abdelmegeed, 2015; Lourenço, 1998). This great variety of constituents is what makes it that masonry becomes heterogeneous in nature; thus, the properties and contents of the masonry vary (Bucknall, 2020; Ellen MacArthur Foundation, 2017).

This study answers a clarion call across the globe on the management of plastic waste, coupled with the demand by the building and construction industry on materials sustainable to the ecosystem. The structural performance under cyclic loading is still quite poorly appreciated in the in-plane, though the potential for applications of recycled plastic is recognized (Rashid et al, 2019; Ramos Huarachi et al, 2020; Desai, 2018).

The use of plastic bricks made of recycled PET, HDPE, and others is potentially applicable in masonry structures according to several studies (Pacheco-Torgal et al, 2018). Certainly, such kind of materials serves the purpose of waste reduction, rather characterized by qualities like improvement in thermal insulation and reduction of overall construction cost. However, the mechanical behavior and the structural integrity when the masonry structures are built with the help of such sophisticated materials do remain underexplored areas requiring suitable research (Lamba et al, 2022).

Composite materials, blending polymeric matrices with ceramic particles, have seen broad application across industries, leveraging the strengths of both components (Abdelhak et al, 2018). Another avenue

explored involves bricks comprising plastics like PET, PP, or HDPE mixed with sand, clay, or brick powder, with studies varying proportions to optimize mechanical and thermal properties. For instance, Kurian et al. experimented with thermocol, plastic, and sand mixtures, observing no water absorption and achieving a peak compressive strength of 11 N/mm² with 25% plastic content (Kurian et al, 2016). Similarly, Kulkarni et al. investigated the compressive strength of HDPE and PP bricks, resulting in strengths of 11.19 N/mm² for HDPE and 10.02 N/mm² for PP, comparable to the 10.5 N/mm² strength of first-class conventional bricks (Kulkarni et al, 2022). Singhal & Netula combined melted PET, LDPE, HDPE, and PP with stone dust, achieving a water-resistant material boasting a compressive strength of 5.6 N/mm² (Mahmoudi, 2014, 2015; Singhal & Netula, 2018).

Youcef et al. examined the reinforcement of brick particles in a PET matrix. Four unique samples, designated C1, C2, C3, and C4, were examined as part of the study. PET constituted a different weight proportion in each sample, ranging from 70%, 65%, 60%, and 55%, respectively. To test the performance of these samples as reinforced composites, their mechanical properties were evaluated. The results showed that compared to the other compositions, the C1 sample produced better results. Therefore, the analysis and potential applications of the C1 sample will be discussed in more detail in the following sections of this study (Moulai Arbi et al, 2023).

Recent literature in numerical tests focuses more on understanding masonry wall behavior under various conditions, spanning experimental and numerical analysis. Celano et al. (2021) focus on the in-plane resistance and design formulations, Choudhury et al. (2020) explore unreinforced masonry components against seismic loads, Radnić et al, (2012) offer a comprehensive numerical model for static and dynamic analyses. Koocheki & Pietruszczak (2023) innovate with artificial neural networks for analyzing large structures. However, these studies primarily focus on traditional materials, and the incorporation of innovative materials like plastic bricks in numerical simulations remains largely unexplored, indicating a potential area for future research in enhancing sustainability and material innovation in masonry construction.

The present numerical study focuses to further explore this avenue and open a way for exploration to be carried out in the case of plastic bricks made up of sand and PET (Polyethylene Terephthalate), providing a different avenue for exploring sustainable materials in construction.

This study helps in deciding the possibility of integrating plastic bricks made from sand and PET (Moulai Arbi et al, 2023), into the masonry wall

using computer software (Abaqus/CAE) (Dassault Systems, The 3DEXPERIENCE platform, 2017) to create a 3D computer model of the masonry wall using plastic bricks instead of the conventional masonry unit. To confirm accuracy, this model is compared to a previous numerical model (Abdulla et al, 2017) and an experimental model (Mojsilović et al, 2009). Python is an open-source programming language used in Abaqus products for customization and scripting (Van Rossum, 1995).

Numerical modeling approaches

Several numerical modeling methods have been developed to simulate the behavior of masonry in both linear and nonlinear states. The most common are the discrete element method (DEM) (Rafiee & Vinches, 2013), the limit analysis (Roca et al, 2010), the applied element method (AEM) (Pandey & Meguro, 2004), and the finite element method (FEM) (Zhai et al, 2017). As it has been mentioned, the numerical model is based on the finite element method and implemented in the Abaqus software, used within the presented work.

The approaches used in masonry by the finite element method generally fall into two categories: micro-modeling and macro-modeling (Abdulla et al, 2017). It chooses the appropriate one depending on the level of accuracy and complexity that is sought. To the extent that the micro-modeling technique is done in detail, the simulation has individual units and mortar as continuous, interfacing with discontinuous elements between units and mortar.

While the detailed micro model in Figure 1a predicts accurate results, the computational requirements limit its use to relatively small masonry components (Petracca et al, 2017). This seeks to decrease some of the pitfalls involved in much more complicated and comprehensive micro-methodologies by adopting a simple and manageable micro-modeling strategy, as presented in Figure 1(b).

In the macro-modelling technique, masonry is modelled as a homogeneous material; see Figure 1(c), without separating individual pieces and mortar. The material attributes are generated with the characteristics of the averaged masonry constituents by a series of continuous elements defining a masonry construction in its entirety (Lourenço, 2002). It is intended to solve somewhat larger and more complicated brick structures, focusing generally on behavior but may not be able to capture detailed failure modes.

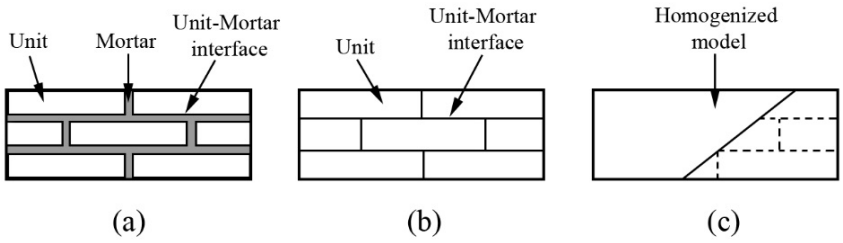

Figure 1 – Finite element modeling approaches (a) micro-detailed model (b) simplified micro-model (c) macro model (Koocheki & Pietruszczak, 2023)

Engineers can safely simulate potentially dangerous or destructive loads and failure scenarios using the finite element analysis (FEA) (Dassault Systems, The 3DEXPERIENCE platform, 2017), allowing them to understand how a system behaves physically at any given time.

It has several advantages, including increased accuracy by examining all potential physical constraints that could affect the design and designers' ability to assess how stresses in one component affect materials in other related parts, leading to better design quality. Early testing during the development phase, where virtual prototypes replace the lengthy and costly process of physical prototyping allows designers to quickly model multiple ideas and materials. The FEA software facilitates the construction of higher-quality products in faster design cycles and with reduced material usage, increasing productivity and revenue. Modeling the interior and exterior of the design will provide more in-depth information about important design factors. This helps designers understand how key elements affect the overall structure and locate potential weak points. Models are efficiently used as one single model can be used to test multiple physical events or failure types. Calculations are fast and initial investment cost low. There is an access to previously collected experimental data that can be used to perform parametric analysis on new models based on previously tested models (Magomedov & Sebaeva, 2020).

It is important to consider the choice of bond pattern when creating a masonry wall model. The stretcher bond, English bond, Flemish bond, and header bond are four distinct bond patterns that need to be considered (see Figure 2). Rows of headers are arranged in header bond with a half-brick offset. Similar to header bond, stretcher bond uses stretchers instead of headers, with the joints in each row centered on a half-brick above and below. By alternating rows of stretchers and headers, where the joints

between the stretchers align with the headers of the lower row, English bond is achieved. In contrast, Flemish bond alternates the arrangement of stretchers and headers in each row, with the stretchers in each row centered on the headers of the lower row, giving the bond a distinctive appearance (Debnath et al, 2023).

In this simulation, the stretcher bond serves as the reference point, as indicated in reference (Abdulla et al, 2017).

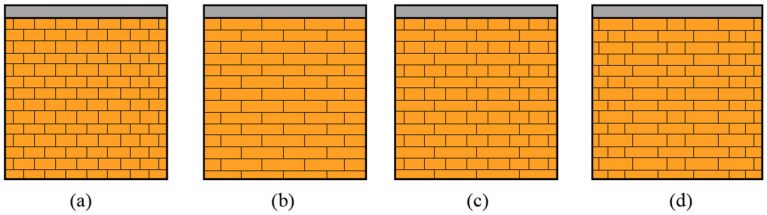

Figure 2 – Masonry bonds, (a) Stretcher bond, (b) Header bond, (c) English bond, (d) Flemish bond (Abdulla et al, 2017)

Five basic types of failure in masonry are represented in Figure 3. The first failure, as shown in Figure 3.a, is considered primarily as a tensile failure, while the second failure is considered a sliding failure by shear, as shown in Figure 3.b. Failure involves shear and diagonal cracking in Figure 3.c, besides masonry crushing failure. Last is the failure marked with cracks, as shown in Figure 3.e. This section focuses on how the computational model was undertaken, providing much detail on how to model the mortar between the two bricks precisely. The model performance is compared with earlier computations and experimental studies reported in the literature for comparison of the present results with those published (Debnath et al, 2023).

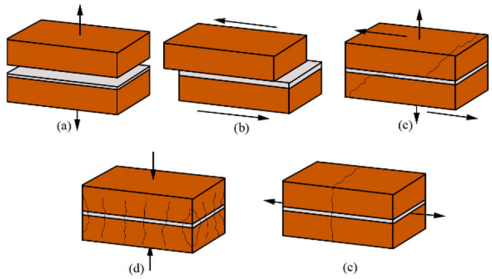

Figure 3 – Failure mechanisms a) tensile failure at the brick-mortar interface, b) shear failure by sliding at the brick-mortar interface, c) diagonal cracking of masonry, d) masonry crushing, and e) tensile cracking between the brick and mortar (Lourenço & Rots, 1997; Sarhosis & Lemos, 2018; Sarhosis et al, 2015)

Methodology description

A simplified micro-modeling technique is used in this study to approximate the three-dimensional responses of masonry specimens. These specimens undergo cyclic loading in the plane controlled by displacement as well as uniaxial compression. Both uniaxial and cyclic tests use displacement in the horizontal direction. Using the finite element modeling (FEM) analysis, the model is constructed in the commercial software Abaqus using solids and interaction surfaces. An application of the damaged plasticity (CDP) concrete model is performed to represent the behavior of masonry components. This model created with Abaqus is capable of reproducing plastic bricks and other quasi-brittle materials, such as the plastic bricks used in this case (Dassault Systems, The 3DEXPERIENCE platform, 2017). Using a surface-based cohesive property, the mortar and the interface between the mortar and masonry units are modeled. This interaction model allows for expressing cohesive connections with thin interfaces (Nela & Grajçevci, 2019).

The modeling approach employed 8-node linear brick (C3D8R) elements to represent the mortar unit, facilitating the capture of complex behaviors within the bricks. Cohesive elements (COH3D8) were utilized to model mortar layers and interfaces, enabling detailed analysis of delamination and crack propagation at brick-mortar joints. Plastic bricks were initially modeled using a linear elastic material model, transitioning to a damage plasticity model to account for post-yield behavior and plastic material characteristics. Similarly, the mortar was described with a damage plasticity model calibrated for its relatively brittle failure and lower tensile strength. Boundary conditions involved support at the base in all directions, with vertical pre-compression loads applied first to simulate self-weight and overhead loads, followed by lateral in-plane loads or cyclic lateral displacements to mimic seismic or wind forces. This sequential loading approach, starting with vertical pre-compression followed by lateral loading, reflects realistic loading conditions and facilitates accurate predictions of stress distribution and failure modes in masonry walls.

Cohesive surface based model for joints

Mathematically, this interaction is encapsulated by an elastic stiffness matrix denoted by "K". This matrix serves as a crucial representation, articulating the linkage between the tensile forces, represented by "t", and the separation vectors, denoted by "δ". The elements within the stiffness matrix "K" are meticulously defined to govern the said relationship, thereby facilitating a precise correlation between the tensile forces exerted and the

resultant vectorial separations. This relationship is succinctly delineated through Equation (1).

Furthermore, the stiffness matrix "K" embodies a pivotal role in the predictive modeling of joint behavior under various loading conditions, offering insights into the mechanical integrity and the failure mechanisms of the joints in question. By delineating the parameters within the matrix "K", researchers and engineers are enabled to simulate and evaluate the structural response of the cohesive interfaces under scrutiny, thus providing a robust framework for the assessment and optimization of material and joint performance within a myriad of engineering applications.

$$\bar{\mathbf{t}} = \begin{Bmatrix} \mathbf{t_n} \\ \mathbf{t_s} \\ \mathbf{t_t} \end{Bmatrix} = \begin{bmatrix} \mathbf{K_{nn}} & \mathbf{0} & \mathbf{0} \\ \mathbf{0} & \mathbf{K_{ss}} & \mathbf{0} \\ \mathbf{0} & \mathbf{0} & \mathbf{K_{tt}} \end{bmatrix} = \bar{\bar{\mathbf{K}}}\bar{\boldsymbol{\delta}} \tag{1}$$

In Equation (1), the terminologies "n", "s", and "t" delineate the normal and shear orientations across the two principal axes. The notation utilizes a single overbar to signify vectors, whereas a double overbar denotes matrices. The stiffness parameters can be articulated through the elastic or shear moduli pertaining to the individual elements and the dimension of the mortar layer, as elucidated in Equations (2) and (3), following the work of Lourenço (1998). Within these equations, "m" and "u" serve to identify the mortar and the unit, correspondingly.

$$\mathbf{K_{nn}} = \frac{\mathbf{E_u E_m}}{\mathbf{h_m}(\mathbf{E_u} - \mathbf{E_m})} \tag{2}$$

$$\mathbf{K_{ss}} = \mathbf{K_{tt}} = \frac{\mathbf{G_u G_m}}{\mathbf{h_m}(\mathbf{G_u} - \mathbf{G_m})} \tag{3}$$

The quadratic stress criterion is useful for the initiation and progression of damage as it indicates the onset of joint degradation, particularly under mixed mode loading. When the quadratic stress ratios of masonry joints reach a value of 1, this condition is considered fulfilled. Equation (4) in Abaqus illustrates the mathematical formulation of this criterion (Abdulla et al, 2017).

$$\left(\frac{\langle t_n \rangle}{t_n^{max}}\right)^2 + \left(\frac{t_s}{t_s^{max}}\right)^2 + \left(\frac{t_t}{t_t^{max}}\right)^2 = 1 \tag{4}$$

In this study, the critical shear stress for joints is regulated by the Mohr-Coulomb failure criteria, and the tensile strength of the joints determines if they undergo tensile cracking.

There are two popular methods for monitoring damage progression: one based on energy and the other on separation. The Benzeggagh-Kenane (BK) formulation is specifically used in the energy-based approach of this study for damage evolution. Equation (5) provides more information on this BK formulation and how it is implemented in Abaqus.

$$\mathbf{G_{IC}} + (\mathbf{G_{IIC}} - \mathbf{G_{IC}}) \left(\frac{\mathbf{G_{shear}}}{\mathbf{G_T}} \right)^{\boldsymbol{\eta}} = \mathbf{G_{TC}} \tag{5}$$

The parameter known as the Exponent, denoted by η, delineates the behavior of the joint, with a value of 2 signifying a brittle characteristic. In essence, an elevated value of η indicates a heightened fragility of the assembly, elevating its vulnerability to abrupt and significant failure.

The energies associated with distinct failure mechanisms within the joints are categorized as Gshear and GT. Gshear amalgamates the energies pertinent to mode III (out-of-plane shear) and mode II (in-plane shear) failure modes of the joint. Concurrently, the energy associated with mode I (tensile) failure mode is integrated with Gshear to constitute GT. These parameters are instrumental in elucidating the joint's response under diverse loading conditions.

Illustrated in Figure 4 is the cohesive behavior of the joints, effectively showcasing the varied reactions of the joint under different loading scenarios and the influence of parameters such as η, Gshear, and GT on such behavior.

Regarding stiffness degradation, it is observed in structural simulations that the stiffness of elements tends to diminish in response to damage or fracture, potentially leading to convergence challenges within the simulation. Convergence is achieved when an analysis yields a stable solution. However, pronounced stiffness degradation may complicate the convergence process, thereby introducing numerical difficulties in the simulation (Nela & Grajçevci, 2019).

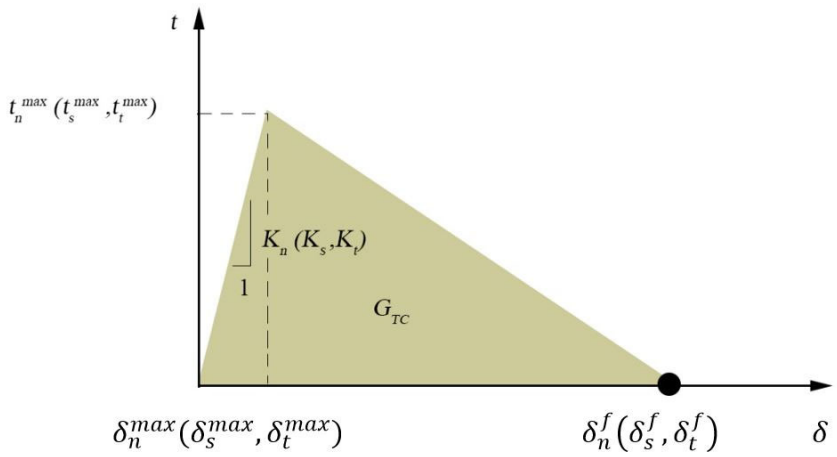

Figure 4 – Traction-separation model for joints (Abdelhak et al, 2018)

Compressive behavior

The Concrete Damage Plasticity (CDP) model uses stress-strain data for compression to characterize the material behavior under compressive pressures. The elastic strain (ε_{0c}^{el}), which represents the strain in the undamaged material (according to Equation 6), is subtracted from the total strain (ε_c) to determine the crushing strain. The model can simulate a reduction in stiffness to represent the material's response when subjected to compression and eventually reaching the crushing point by including a compression damage parameter (dc).

$$\boldsymbol{\varepsilon_c^{in} = \varepsilon_c - \varepsilon_{0c}^{el}}; \tag{6}$$

where $\boldsymbol{\varepsilon_{0c}^{el} = \frac{\sigma_c}{E_0}}$,

a damage parameter that, under compression conditions, varies from 0 (indicating no weakening) to 1 (indicating total weakening or failure). Based on the relationship shown in Equation (7), Abaqus software handles this by automatically translating inelastic strain into plastic strain (ε_c^{pl}). Here, "c" specifically represents compression. This procedure explains the degree of damage that the material undergoes and explains how it plastically reacts to compression.

$$\boldsymbol{\varepsilon_c^{pl} = \varepsilon_c^{in} - \frac{d_c}{(1 - d_c)} \frac{\sigma_c}{E_0}} \tag{7}$$

Tensile behavior

The Concrete Damage Plasticity (CDP) technique uses a softening curve to represent the tensile behavior. This curve illustrates how a material reacts to failure or cracking. In CDP, the deterioration of the elastic modulus (E_0) of the material is what causes this post-failure behavior.

This post-failure behavior is the result of the relationship between the post-failure stress and the crack strain (ε_t^{ck}). According to Equation (8), the crack strain is determined as the difference between the elastic strain (ε_{0t}^{el}) and the total strain (ε_t), where the elastic strain (ε_{0t}^{el}) reflects the strain in the undamaged material.

The model takes into account the decrease in stiffness that occurs when the material starts to crack under stress by including a tension damage parameter (dt). The tension damage parameter ranges from 0 (indicating no loss of strength) to 1 (indicating total loss of strength or failure). This feature helps us understand how the material reacts to tension while considering the degree of damage it has undergone.

$$\boldsymbol{\varepsilon_t^{ck} = \varepsilon_t - \varepsilon_{0t}^{el}}, \tag{8}$$

where $\boldsymbol{\varepsilon_{0t}^{el} = \sigma_t / E_0}$.

However, another method of modeling tensile behavior uses fracture energy (G_t) to describe the decrease in strength after cracking (as seen in Figure 5). Based on the provided fracture energy data, there is a linear loss of strength in this model upon fracture. The fracture energy and the tensile strength (σ_t) of the material are used to calculate the crack displacement (u_{t0}), which indicates the point where the material completely loses its strength. The subscript "t" specifically refers to tension in this case.

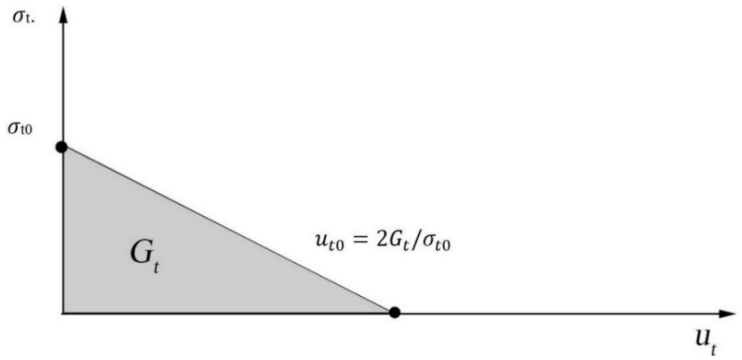

Figure 5 – Post-failure fracture energy curve (Abdelhak et al, 2018)

The effective stress concept in the CDP model relates the actual stress σ to the effective stress $\tilde{\sigma}$ through $\sigma = (1-d)\tilde{\sigma}$ where d is dc or dt. The stress-strain relationship for the damaged material is given by $\sigma = (1-d)E(\epsilon - \epsilon_p)$, with E as the undamaged Young's modulus, ϵ as the total strain, and ϵ_p as the plastic strain. The evolution of dc and dt can be defined as functions of equivalent plastic strains, ϵ_{pl}^c and ϵ_{pl}^t , respectively, often calibrated with experimental data, where $\epsilon_{pl}^c = \frac{\sigma}{E}(1-d_c)$ and $\epsilon_{pl}^t = \frac{\sigma}{E}(1-d_t)$. These relationships illustrate how damage evolves and influences the structural integrity under various loading conditions.

Masonry wall model

The units interact both linearly and nonlinearly considered in this three-dimensional finite element micromodel developed. For this, a consistent strategy based on surface modeling was adopted that would model how the joints were interacting. Discretizing nodes into surfaces and with a finite sliding formulation defined contacts between the neighboring masonry blocks. In the present model, specifically, the behavior of hard contact was implemented, wherein the pressure was transmitted between the surfaces in contact with each other in such a way that there is no penetration of tensile stress and transmission of tensile stress through the contacting surfaces. This resembles quite closely the behavior of the masonry unit surfaces in practice. They tested the validity of the proposed model by comparing its results to the experiments presented by (Mojsilović et al, 2009).

The tests were, therefore, carried out to evaluate the masonry behavior under in-plane cyclic loading (in in-seismic loading conditions) and in-plane monotonic loads. The tested walls had a nominal thickness of 110 mm, a length of 1200 mm, and a height of 1200 mm (see Figure 6). The walls were made of plastic bricks with the following dimensions: length: 230mm, height: 76mm, and thickness: 110mm. The mortar joints had a thickness of 10 mm, and the cement, lime, and sand were mixed in a ratio of 1:1:6. There were a total of 14 rows of bricks, with 5 bricks per row, arranged in a common bond pattern in each wall.

In our study, the scale ratio used for the test specimens is 1:1, meaning that the models are full-scale. The choice of full-scale specimens ensures that the results are directly applicable to real-world scenarios, providing a more accurate representation of the behavior and performance of masonry structures under various loading conditions. Utilizing full-scale

specimens eliminates the need to account for scaling effects, which can introduce additional variables and potential inaccuracies in the analysis.

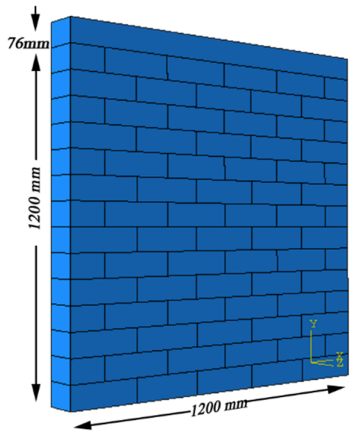

Figure 6 – Numerical model of the masonry wall.

Properties

In this illustration, the response of the wall to seismic conditions and in-plane loads reproduced above is modeled using Abaqus software, as described earlier. It had simplified brick micro-modeling assembling techniques with the mortar taken as an interaction parameter. Both cohesive behavior and damage behavior are included in these interaction characteristics.

Table 1 shows the properties of the plastic bricks. The designed geometric shapes for the plastic bricks were done in the 3D modeling environment. The bricks were represented as solid objects in order to best represent the characteristics of the designed objects. It can be obtained from the table that the characteristics of the plastic bricks are 1660 kg/m^{3}for density, 2771 MPa for Young's modulus, and 0.3 for Poisson's ratio (Moulai Arbi et al, 2023).

Table 1 – Properties of the plastic bricks (Moulai Arbi et al, 2023)

Density (kg/m^3)	Young's modulus (MPa)	Poisson's ratio
1660	2771	0.3

In this study, the Drucker-Prager model describes the plasticity characteristics found on the mechanical menu. In the same menu, more specifically in the plasticity zone, was the Drucker-Prager model. The model is designed with a friction angle of 36 degrees, a flow stress ratio of 1, and a dilation angle of 11.3 degrees, as shown in Table 2. It also hardens at 14.18 MPa on Drucker-Prager F. et al. (Abdulla et al, 2017) identified mortar properties, which are presented in Tables 2 and 3.

Table 2 – Properties of Drucker-Prager (Abdulla et al, 2017)

Friction angle (β)	Flow stress ratio (R)	Dilation angle (ψ)
36	1	11.3

The described construction technique delineates a masonry wall comprising 14 rows of bricks. This approach eschews the portrayal of mortar as an independent entity, opting instead for a detailed crafting and assembly of each brick. Within the Abaqus software framework, the attributes of the mortar find their representation through interaction properties.

The mechanical menu's normal behavior category specifies a friction coefficient (μ) of 0.75 (Raijmakers, 1992). Furthermore, the model incorporates cohesive behavior, encompassing the parameters Knn, Ktt, and Kss as delineated in Table 3. These parameters, Knn for the normal direction stiffness, Kss for the shear direction stiffness, and Ktt for the secondary shear direction stiffness, collectively articulate the stiffness properties of the mortar.

Table 3 – Joint interface properties (Abdulla et al, 2017)

Knn (n/mm^3)	Kss (n/mm^3)	Ktt (n/mm^3)
63	25	25

Table 4 outlines the parameters for mechanical behavior, selecting the tension damage option and assigning it a threshold of 0.2 MPa, as detailed in the literature (Abdulla et al, 2017). The chosen framework for damage analysis is the Benzagagh-Kenan model, with a specified value of 2 signifying a tendency towards brittle characteristics, in accordance with the findings in (Benzeggagh & Kenane, 1996).

For the first and second shear modes, the designated rupture energy is 0.04 N/mm (Lourenço, 2002), whereas the energy for normal rupture is established at 0.012 N/mm (Angelillo et al, 2014).

Table 4 – Properties of the masonry wall (Abdulla et al, 2017).

Friction coef (μ)	Tension t_n^{max} (MPa)	B-K	G_{IC} (N/mm)	G_{IIC} (N/mm)
0.75	0.2	2	0.012	0.04

In the Concrete Damage Plasticity (CDP) model used in Abaqus, the parameters ω_c and ω_t are dimensionless factors representing the reduction in stiffness due to damage under compressive and tensile loading, respectively. Specifically, ω_c is typically set to 0.9 and ω_t to 0.7, indicating that the stiffness in compression and tension is reduced by 10% and 30% respectively when the material is fully damaged. These parameters are integrated into the model through effective stress relationships: $\sigma = (1 - d.\omega_c)\tilde{\sigma}_c$ for compression and $\sigma = (1 - d.\omega_t)\tilde{\sigma}_t$ for tension, where $\tilde{\sigma}_c$ and $\tilde{\sigma}_t$ are the effective stresses. The damage parameters d_c and d_t evolve based on equivalent plastic strains, reflecting the material's degradation and ensuring accurate simulation of cyclic loading behavior.

Meshing module

Meshing, a pivotal step in the finite element analysis, entails the subdivision of a structure into myriad diminutive elements. These elements are individually computed, and aggregating their computational outcomes yields the structure's final analysis result.

This analytical process bifurcates into three principal segments: pre-processing, processing, and post-processing. During pre-processing, based on the chosen analytical framework, be it modal analysis or structural static analysis, the requisite element type is determined. This stage involves the establishment of nodes, allocation of material properties, application of boundary conditions and loads, and the fabrication of elements by linking them with nodes (Kumar, 2022).

The processing phase unfolds within the computational domain, where the software undertakes the resolution of the boundary value problem, subsequently presenting the results for user review.

In the post-processing phase, the analyst evaluates the derived results, focusing on metrics such as temperature variations, displacements, durations, stresses, strains, and natural frequencies (Magomedov & Sebaeva, 2020).

A mesh sensitivity investigation was conducted to ascertain the optimal mesh size for an accurate stress analysis in a masonry wall subjected to numerical evaluation. The initial analysis utilized a mesh

configuration of 7 X 2 X 3 elements per masonry unit, mirroring the unit's dimensions of 110 mm in thickness, 76 mm in height, and 230 mm in length, as depicted in Figure 7a. The subsequent analysis increased the mesh density by employing a 7 X 4 X 3 element arrangement for each unit, effectively augmenting the element count, as illustrated in Figure 7b. The final phase of the analysis quadrupled the element number from the initial setup by adopting a 7 X 4 X 6 element scheme for each unit, as shown in Figure 7c (Abdulla et al, 2017).

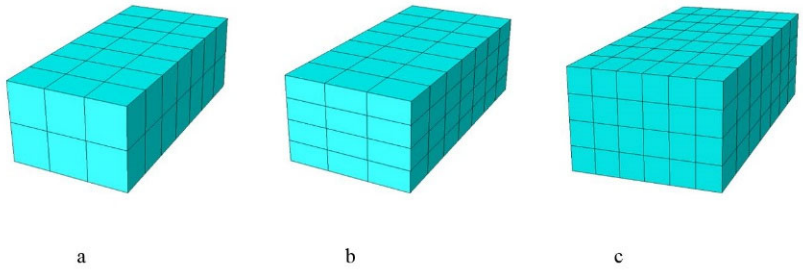

Figure 7 – Mesh sizes used in masonry units.

In the mesh module depiction of the complete masonry wall assembly, as showcased in Figure 8, the configuration with a 7 X 2 X 3 elements mesh comprises a total of 8,136 nodes and 3,600 elements. This detailed representation underscores the intricate network of computational points and structural components that constitute the analytical model of the wall.

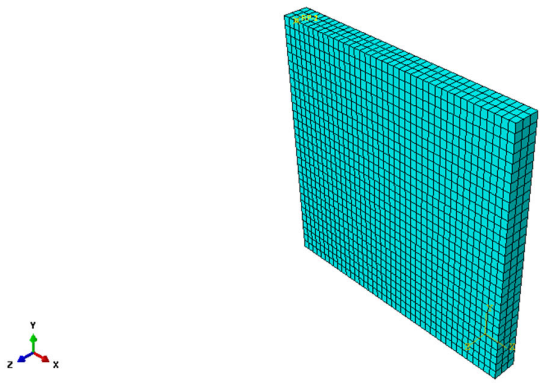

Figure 8 – Comprehensive Mesh Structure of a Masonry Wall Model: 7 X 2 X 3 Element Configuration

Figure 9 reveals that across all tested scenarios, the outcomes regarding failure modes and the elastic and plastic behaviors remained consistent. This analysis underscores the minimal sensitivity of the proposed model to variations in mesh granularity. Consequently, the adoption of coarser mesh configurations is feasible, offering the benefit of substantially decreased computational demands.

The computational time associated with each mesh configuration was a paramount consideration, given the extensive nature of our simulations. The finest mesh (7X4X6 elements) needed 110 minutes, which was the highest computational investment. On the other hand, the intermediate mesh (7X4X3 elements) required 80 minutes, and the lowest computational investment of 50 minutes was for the coarsest mesh (7X2X3 elements).

Rationale for mesh selection

The decision to opt for the coarsest mesh configuration (7X2X3 elements) was based on key findings from the sensitivity analysis. The results showed comparable accuracy across mesh densities, indicating that finer meshing would not significantly improve accuracy. Additionally, the coarsest mesh offered significant computational efficiency, with a reduction in computational time from 110 to 50 minutes, facilitating wider model utilization for large-scale parametric studies without proportional increases in computing resources.

This configuration struck an optimal balance between computational manageability and detail, ensuring sufficient capture of nuanced structural behavior, including crack initiation and propagation, critical for assessing wall strength under various loading conditions.

The applied actions, whether load or displacement, to the model during the numerical analysis were made successively. This indicates that the applied actions were actually gradually imposed actions on the model, as it may relate to the load or the displacement control.

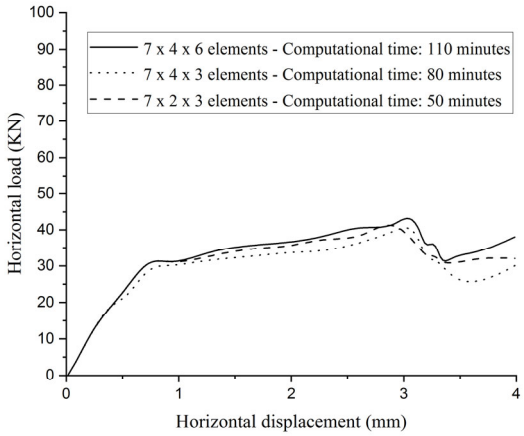

Figure 9 – Comparison between different mesh sizes.

Loads

Figure (10) shows a schematic of the experimental setup carried out in the investigation of the performance of masonry walls under horizontal cyclic loads in structural engineering. The test specimen itself, usually a masonry wall built from individual bricks or blocks, is at the heart of this system. The latter then serves to carry out a simulation of the real-life stresses, from which the wall might suffer during its service life. An actuator, a high-end device used to apply controlled loads or displacements, applies horizontal forces.

This actuator can apply the required load with not only the static, but also dynamic and cyclic loads that can be produced by environmental conditions, such as earthquakes or wind. Sensing devices are placed at strategic points on the wall and the actuator for measuring response to the loads. These sensors may be strain gauges, displacement transducers, or load cells to get real-time information of the recorded stresses, strains, and deformations at the wall.

The numerical work attempts to replicate the conditions of loading imposed on the masonry wall with realism inside the simulated environment. From the corresponding physical tests, the horizontal and cyclic loads are applied on the walls of masonry having the same characteristics (Rezapour et al, 2021).

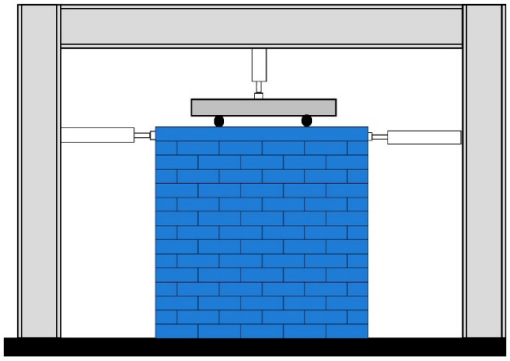

Figure 10 – Experimental masonry wall under loads

In-plane loading

The wall received a controlled vertical compressive load from the top of the beam. After setting the compressive load, it restricted the upper beam's vertical movement. Subsequently, it applied a gradual and monotonic horizontal load to the wall through the upper beam (Figure 11).

Executed in two stages, the numerical analysis first introduced the initial vertical compression load. The second phase proceeded under the identical boundary conditions as the experiment, but it added restrictions to prevent out-of-plane vertical and horizontal displacements and rotations at the top of the wall around all axes. Throughout this phase, the approach maintained the vertical compressive stress while incrementally applying the horizontal load in the plane under displacement control (Abdulla et al, 2017).

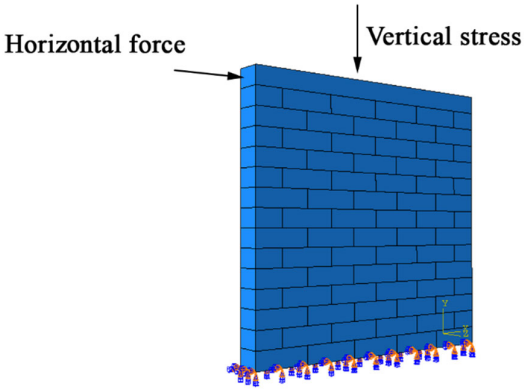

Figure 11 – Brick wall with loading in the plane

In-plane cyclic loading

In the numerical simulation detailed in Figure 12, the wall was subjected to a sequence of loading phases, beginning with a vertical compression load applied from the top, whereupon the vertical movement of the upper beam was restricted. This initial stage, termed the pre-compression phase, involved maintaining a constant vertical stress before transitioning to the second stage. During this subsequent phase, the wall, now stabilized under displacement control, was subjected to progressive cyclic horizontal loads within the plane. This methodology encapsulates a comprehensive approach to evaluating the structural response of the wall under varying load conditions, thereby enabling a detailed analysis of its behavior in a controlled numerical environment (Abdulla et al, 2017).

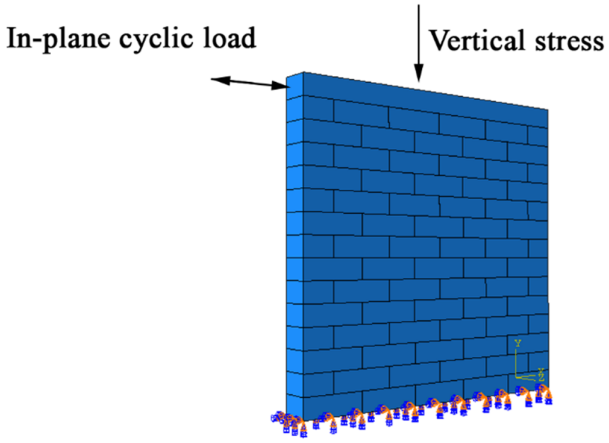

Figure 12 – Masonry wall subjected to cyclic loading in the plane

The study encompassed 19 loading cycles on a specifically selected wall, which had been subjected to an initial vertical stress of 0.7 MPa. Figure 13 illustrates the detailed load distribution patterns exerted on the wall top. This wall, uniquely identified within the experimental setup as A3-1, stood as the focal point of our investigation, offering insights into the stress response and structural behavior under the applied loading conditions (Magomedov & Sebaeva, 2020).

Data points (x, y) were collected using OriginLab (2020) and subsequently imported into Abaqus for analysis. These data, derived from cyclic loading experiments, are compiled and presented in Table 5. It displays the outcomes and patterns observed from the loading cycles.

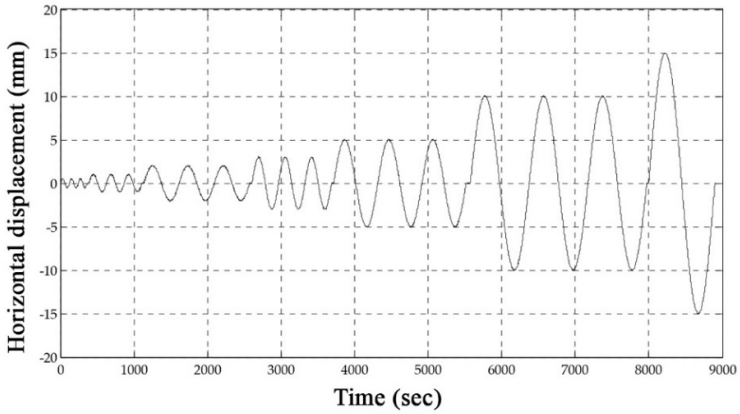

Figure 13 – Displacement loading history (Magomedov & Sebaeva, 2020)

Results

In-plane loading

The graph in Figure 14 presents a comparison of the numerical results between two types of masonry walls: one constructed with plastic bricks and another from a study by (Abdulla et al, 2017), which presumably uses traditional masonry materials.

As the horizontal displacement increases, both lines show an initial steep incline, indicating that the load capacity increases with displacement up to a certain point. This portion of the curve represents the elastic behavior of the materials where the deformation is proportional to the load and is recoverable.

However, as the displacement continues to increase, both lines plateau and exhibit peaks, representing the maximum load capacity of the walls. Beyond these peaks, the lines fluctuate and generally trend downwards, indicative of the walls experiencing damage and undergoing inelastic deformation, where the bricks are likely to have yielded or the mortar have cracked, leading to a decrease in load capacity.

The results showed consistency and good agreement in terms of failure modes. It is interesting to note that the masonry wall constructed from plastic bricks has a lower horizontal load capacity compared to the masonry wall developed by Kurdo F. et al. For example, in Kurdo F. et al.'s study, the maximum load for the masonry wall was 55.40 kilonewtons (KN), while the maximum load observed for the masonry wall using plastic bricks reached 39.10 KN (Abdulla et al, 2017).

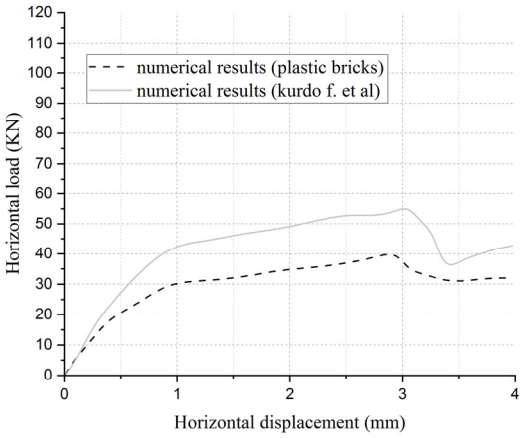

Figure 14 – Horizontal load-displacement comparison

Table 5 represents a quantitative summary of the horizontal load capacities for the two numerical models of masonry walls subjected to incremental horizontal displacements.

Table 5 – Numerical data of the wall under in-plane loading

	Horizontal displacement (mm)	0	0.5	1	1.5	2	2.5	3	3.5	4
Horizontal loads (Kn)	Plastic bricks	0	21.27	29.82	31.86	34.94	36.30	36.67	30.84	32.19
	(Abdulla et al, 2017)	0	27.75	42.81	46.24	49.33	52.75	55.40	37.35	43.15

Figure 15 depicts a comparison between the experimental results of a traditional masonry wall and the numerical simulations for plastic bricks walls, examining their behavior under horizontal loading (Vargas et al, 2023). The numerical simulation closely mirrors the trend exhibited by the experimental results, demonstrating good agreement in terms of the overall shape and peak values of the load-displacement curve. Initially, both lines ascend steeply, indicating a linear increase in load with displacement, characteristic of the elastic behavior of the wall where deformation is recoverable upon load removal. As displacement continues, both curves reach a peak point. The convergence of the two curves validates the numerical model, confirming that it is a reliable predictor of the experimental wall's behavior (Raijmakers, 1992).

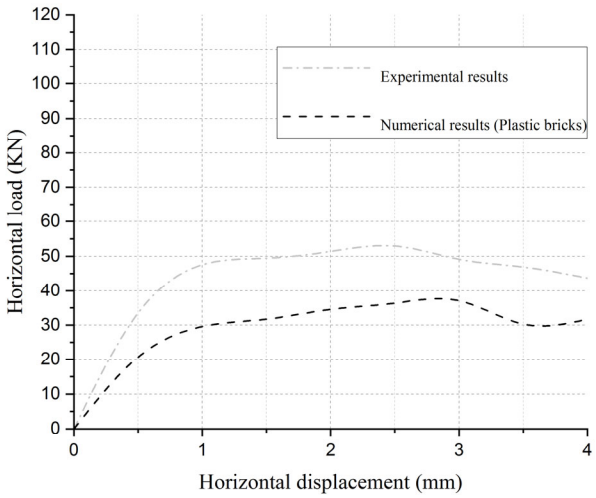

Figure 15 – Comparison between the numerical and experimental results

Table 6 presents a comparative analysis of the load capacities between a numerically modeled plastic brick masonry wall and an experimentally tested wall composed of traditional bricks across a range of horizontal displacements. The table reveals that at every displacement point, the traditional brick wall exhibits a superior load capacity compared to the plastic brick wall, with a pronounced difference at the peak load point 52.93 kN for the traditional brick wall versus 36.30 kN for the plastic brick wall at 2.5 mm displacement.

This comparison highlights the divergence in structural performance between the two materials, emphasizing the higher load-bearing efficiency of traditional bricks over their plastic counterparts.

Table 6 – Data results of the numerical and experimental work

	Horizontal displacement (mm)	0	0.5	1	1.5	2	2.5	3	3.5	4
Horizontal loads (Kn)	Plastic bricks	0	21.27	29.82	31.86	34.94	36.30	36.67	30.84	32.19
	Experimental results	0	33.51	47.53	49.42	51.36	52.93	49.14	46.89	43.70

The disparity in load capacity between the plastic brick masonry wall and a traditional masonry wall can be attributed to distinct material properties and the interaction between components within the wall system.

Plastic bricks generally exhibit a lower modulus of elasticity compared to traditional masonry materials, which contributes to a reduced capacity to withstand loads before deforming. The compressive strength of plastic bricks also tends to be less than that of traditional bricks, leading to a decrease in overall load-bearing capability (D'Altri et al, 2020). The bonding between plastic bricks and mortar is typically weaker than that of traditional brick-and-mortar joints, which can result in a lower horizontal load capacity for walls constructed with plastic bricks. Unlike traditional masonry materials, which are often brittle, plastic materials are more ductile, meaning they can undergo more extensive deformation under load, a characteristic that can lower the peak load capacity of a wall due to the material yielding at lower stress levels.

In Figure 16, "STATUSXFEM" represents the extent of fracturing within the individual elements of the masonry wall model. A full fracture within an element is indicated by a status value of 1, while a status of 0 signifies an absence of cracking. The values falling between 0 and 1 denote varying degrees of partial element fractures. The inception of tensile fractures was noted at the base of the wall as the loading commenced, which precipitated the compression and subsequent buckling of the wall lower regions. This sequence of stress response gave rise to diagonal fracturing that propagated between the blocks, leading to further cracking within the blocks themselves.

The depicted diagonal crack pattern corresponds to one of the observed failure modes in experimental settings, known as diagonal failure, which is a common mode of failure in masonry structures subjected to lateral forces (Ponte et al, 2019). Additionally, the analysis revealed both vertical and horizontal slippage occurring among the plastic brick units, contributing to the overall degradation of the wall structural integrity under stress (Ghiassi et al, 2012; Zhang et al, 2023).

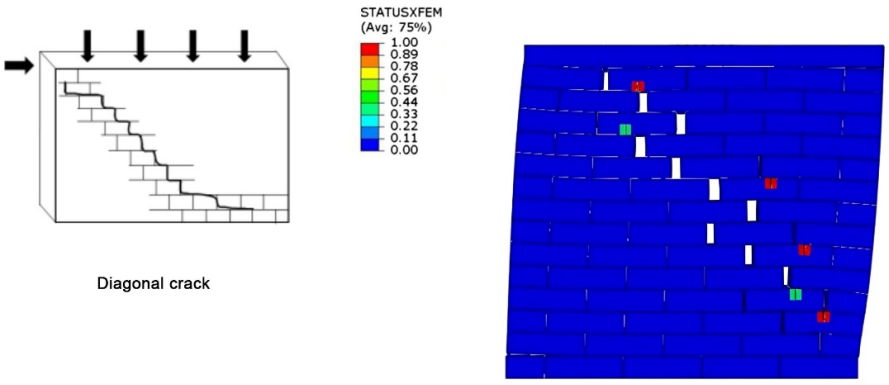

Figure 16 – Failure pattern of the masonry wall

In-plane cyclic loading

Cyclic loading graphs are instrumental in analyzing the dynamic response of structures, such as walls, during seismic events (Xia et al, 2024). The graph in Figure 17 representing force over time is derived from the numerical simulation of the plastic brick wall that subject a masonry wall to cyclical loading, mimicking the push-pull effects encountered during an earthquake. It charts the force exerted on the wall, measured in exponential units, as it oscillates over time.

By synthesizing data from the displacement loading history in Figure 12 and data from force loading history in Figure 16, a hysteresis loop can be constructed (Krtinić et al, 2023), which is a powerful tool for visualizing the energy dissipation and the cyclic stiffness degradation of the wall under seismic loading (Figure 17).

A hysteresis loop graph exhibits the relationship between load and displacement for each cycle, highlighting the wall energy dissipation capacity, an essential factor in seismic design. This capacity is crucial for quantifying how a structure absorbs and releases energy, which directly impacts its ability to withstand and recover from earthquake-induced stresses. The required computational time for the masonry wall under cyclic load is 130min.

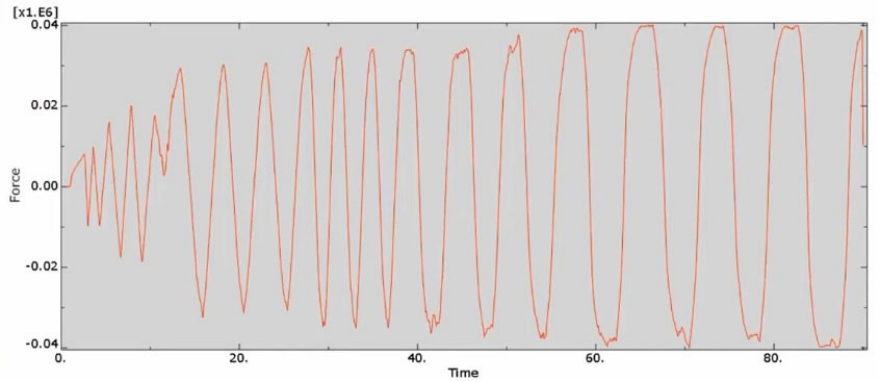

Figure 17 – Force loading history

The hysteresis graphs in Figure 18 provide a side-by-side evaluation of the experimental and computational responses of a masonry wall subjected to cyclic loading. In the comparison, it is noteworthy that the experimental model withstood a higher peak for horizontal force, reaching 45.53 kilonewtons (kN), in contrast to the numerical model, which peaked at 34.20 kN.

This discrepancy suggests that the numerical model predicted an earlier onset of horizontal slides along the lower course of the masonry units. The predominant failure mechanism in the simulation was horizontal cracking along the lower mortar joints. Furthermore, vertical slippage was a prominent feature at the base of the wall in the simulation data(Rahim et al, 2024).

The sequence from A to D in Figure 19 illustrates the escalating stress response of a masonry wall subjected to cyclic loading, as depicted by the von Mises stress distribution. The panel A shows initial stress at the wall base. As the cyclic loading progresses, the panels B and C reveal a significant increase in stress towards the center, signaling higher stress levels likely leading to material deformation. The panel D exhibits the culmination of stress throughout the wall, with the most intense stress (red areas) indicating failure.

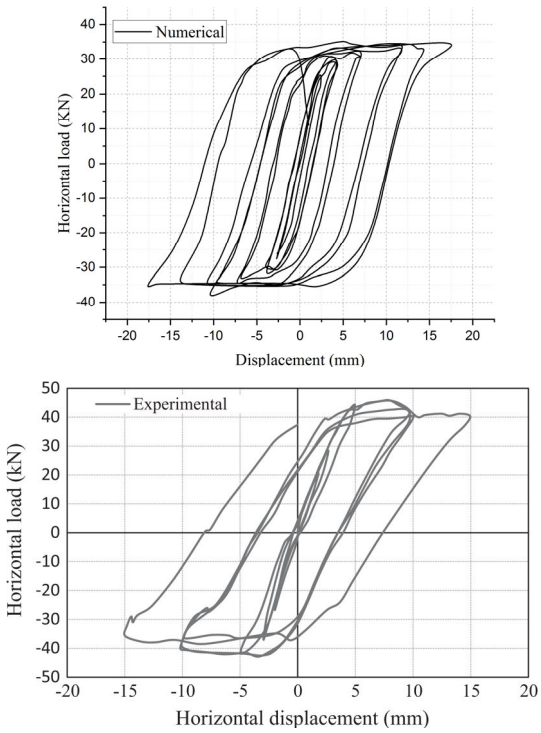

Figure 18 – Comparison between numerical and experimental cyclic loading in the plane.

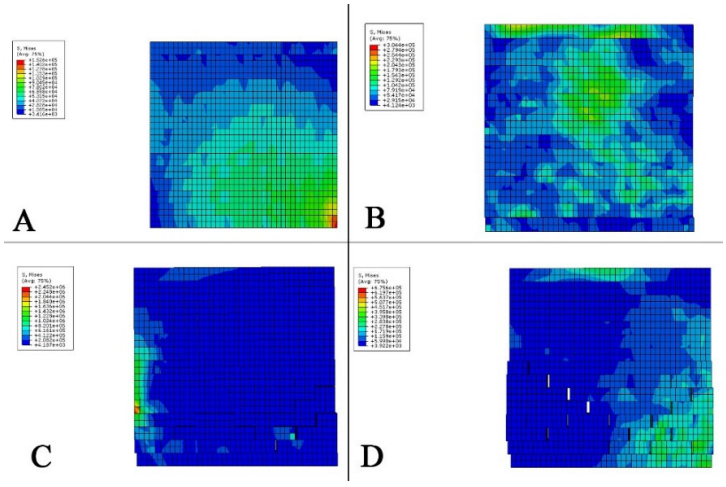

Figure 19 – Stress response of the masonry wall under cyclic loading

The four panels, labeled A to D, in Figure 20 depict the displacement progression of a masonry wall subjected to cyclic loading, revealing the deformation pattern and identifying the areas where sliding occurs between the brick units. The panel A starts with minimal displacement, and as the panels progress to D, there is a significant increase in displacement magnitude, especially evident in the lower sections of the wall.

The panel B shows the beginning of sliding in the bottom line of units, indicating a shift in the structural integrity of the wall. In the panel C, the beginning of diagonal failure occurs, suggesting increased stress concentration within the masonry structure.

The panel D shows a pronounced displacement pattern that closely resembles the diagonal tension failure observed in experimental studies (Figure 21), characterized by a distinct diagonal crack pattern within the wall. This failure mode is indicative of bricks sliding past each other, leading to a loss of cohesion in the masonry structure and the formation of cracks along the lines of maximum shear stress. The final panel D, mirroring the experimental diagonal tension failure mode, reflects a critical state where significant displacement leads to structural failure.

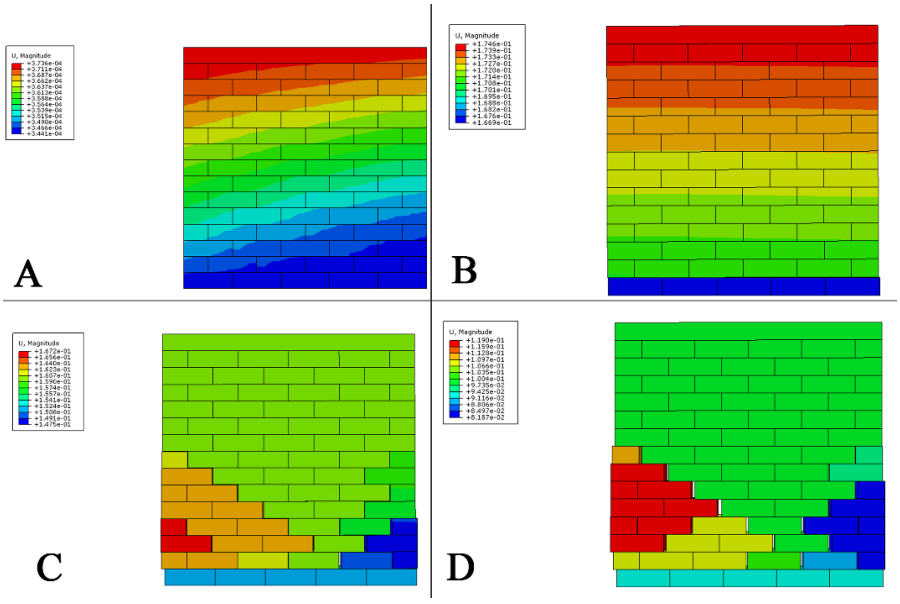

Figure 20 – Displacement progression of a masonry wall under cyclic loading

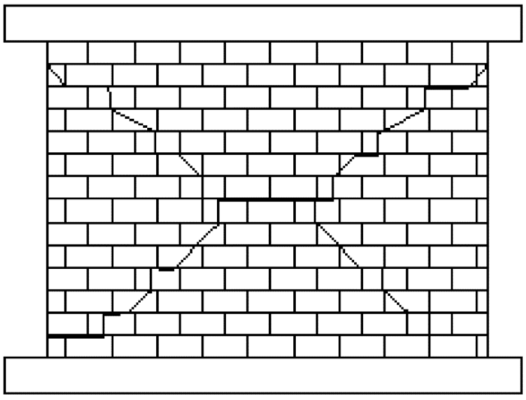

Figure 21 – Diagonal tension failure mode (Choi et al, 2023)

In addressing the comparative analysis between our numerical models and the experimental data, our investigation reveals a nuanced correlation that underscores the utility of numerical simulations in replicating the complex behaviors of masonry walls constructed with recycled plastic bricks under in-plane loading. The numerical results showcased in "Table numerical data of wall under in-plane loading" and the experimental findings presented in "Table data results of numerical and experimental work" elucidate a substantial degree of concordance, particularly in capturing the trend of load capacity against displacement. Despite the observed quantitative discrepancies, such as a lower peak load capacity in numerical predictions (36.67 kN for numerical vs. 49.14 kN experimentally at a 3 mm displacement), the numerical model effectively mirrors the overall shape of the experimental load-displacement curve. This indicates that the model adeptly captures the essential mechanical response of masonry walls, albeit with conservative estimates of peak strengths. Notably, the early onset of nonlinear behavior in numerical simulations compared to experimental observations suggests model sensitivity to material property assumptions and boundary conditions, highlighting areas for refinement. The critical examination of failure modes, where numerical analysis predicts horizontal cracking along lower mortar joints akin to experimental results, further validates the relevance of the model in simulating real-world phenomena. This qualitative agreement emphasizes the potential of the model as a predictive tool, albeit necessitating adjustments in material

characterization and enhanced detailing of the brick-mortar interface to amplify its accuracy and predictive power.

Conclusion

The numerical modeling study presented here offers a critical exploration into the structural performance of masonry walls utilizing recycled plastic bricks subjected to both in-plane and cyclic loading conditions. The analysis, conducted through a simplified micro-modeling approach in Abaqus, provides a foundational understanding of the mechanical behaviors and failure mechanisms associated with this innovative construction material. The study's findings elucidate a lower load-bearing capacity of walls constructed with plastic bricks when compared to their conventional counterparts, alongside an earlier onset of damage under cyclic loading scenarios. Notably, the emergence of horizontal cracking along lower mortar joints and the observation of diagonal failure modes and sliding, particularly at the wall base under cyclic loads, underscore the distinct structural responses of these materials under stress.

The practical significance of this research lies in its contribution to the broader field of sustainable construction practices. By demonstrating the feasibility of employing recycled plastic bricks in masonry wall construction, this study paves the way for their consideration in non-load-bearing applications and highlights their potential in contributing to waste reduction and environmental sustainability in the construction industry. Furthermore, the nuanced understanding of failure mechanisms and load-bearing behaviors garnered through this numerical modeling offers valuable insights for the development of design guidelines and the optimization of plastic brick formulations to enhance their structural performance.

In conclusion, while recycled plastic bricks present a reduction in strength compared to traditional masonry materials, their incorporation into construction projects represents a viable path toward achieving more sustainable building practices. The outcomes of this research not only advocate for the innovative use of waste materials in construction but also lay the groundwork for future investigations aimed at refining the structural capabilities and application scope of plastic bricks, thereby reinforcing the imperative of sustainability in the built environment.

References

Abdelhak, B., Mahmoudi, N. & Hacen, M. 2018. Improvement of the Interfacial Adhesion Between Fiber and Matrix. *Mechanics and Mechanical Engineering,* 22(4)**,** pp.885-893.

Abdelmegeed, M.M.A 2015. *Damage assessement and rehabilitation of historic traditional masonry*. PhD thesis. Athens, Greece: National Technical University of Athens (NTUA), Faculty of civil engineering [online]. Available at: https://www.fayoum.edu.eg/Arc/Restoration/pdf/MrMohamedPhd.pdf [Accessed: 21 April 2024].

Abdulla, K.F., Cunningham, L.S. & Gillie, M. 2017. Simulating masonry wall behaviour using a simplified micro-model approach. *Engineering Structures,* 151**,** pp.349-365. Available at: https://doi.org/10.1016/j.engstruct.2017.08.021.

Angelillo, M., Lourenço, P.B., Milani, G. 2014. Masonry behaviour and modelling. In: Angelillo, M. (Eds.) *Mechanics of Masonry Structures*. *CISM International Centre for Mechanical Sciences*, 551, pp.1-26. Vienna: Springer. Available at: https://doi.org/10.1007/978-3-7091-1774-3_1.

Benzeggagh, M.L. & Kenane, M. 1996. Measurement of mixed-mode delamination fracture toughness of unidirectional glass/epoxy composites with mixed-mode bending apparatus. *Composites Science and Technology,* 56(4)**,** pp.439-449. Available at: https://doi.org/10.1016/0266-3538(96)00005-X.

Bucknall, D.G. 2020. Plastics as a materials system in a circular economy. *Philosophical Transactions of the Royal Society A,* 378(2176)**,** art.number:20190268. Available at: https://doi.org/10.1098/rsta.2019.0268.

Celano, T., Argiento, L.U., Ceroni, F. & Casapulla, C. 2021. In-Plane Behaviour of Masonry Walls: Numerical Analysis and Design Formulations. *Materials*, 14(19), art.number:5780. Available at: https://doi.org/10.3390/ma14195780.

Choi, H., Quan, C. & Jin, K. 2023. Nonlinear Performance Curve Estimation of Unreinforced Masonry Walls Subjected to In-Plane Rocking Behavior. *Applied Sciences,* 13(12)**,** art.number:7298. Available at: https://doi.org/10.3390/app13127298.

Choudhury, T., Milani, G. & Kaushik, H.B. 2020. Experimental and numerical analyses of unreinforced masonry wall components and building. *Construction and Building Materials,* 257**,** art.number:119599. Available at: https://doi.org/10.1016/j.conbuildmat.2020.119599.

D'altri, A.M., Sarhosis, V., Milani, G., Rots, J., Cattari, S., Lagomarsino, S., Sacco, E., Tralli, A., Castellazzi, G. & de Miranda, S. 2020. Modeling Strategies for the Computational Analysis of Unreinforced Masonry Structures: Review and Classification. *Archives of Computational Methods in Engineering,* 27**,** pp.1153-1185. Available at: https://doi.org/10.1007/s11831-019-09351-x.

-Dassault Systems, The 3DEXPERIENCE platform. 2017. *Simulia: Abaqus Finite Element Analysis for Mechanical Engineering and Civil Engineering* [online]. Available at: https://www.3ds.com/products/simulia/abaqus [Accessed: 21 April 2024].

Debnath, P., Chandra Dutta, S. & Mandal, P. 2023. Lateral behaviour of masonry walls with different types of brick bonds, aspect ratio and strengthening measures by polypropylene bands and wire mesh. *Structures*, 49, pp.623-639. Available at: https://doi.org/10.1016/j.istruc.2023.01.155.

Desai, B.H. 2018. 14. United Nations Environment Program (UNEP). *Yearbook of International Environmental Law,* 32(1)**,** pp.293-298. Available at: https://doi.org/10.1093/yiel/yvac039.

-Ellen MacArthur Foundation. 2017. The New Plastics Economy: Rethinking the future of plastics & catalysing action. *Ellenmacarthurfoundation.org* [online]. Available at: https://www.ellenmacarthurfoundation.org/the-new-plastics-economy-rethinking-the-future-of-plastics-and-catalysing [Accessed: 21 April 2024].

Ghiassi, B., Marcari, G., Oliveira, D.V. & Lourenço, P.B. 2012. Numerical analysis of bond behavior between masonry bricks and composite materials. *Engineering Structures,* 43**,** pp.210-220. Available at: https://doi.org/10.1016/j.engstruct.2012.05.022.

Koocheki, K. & Pietruszczak, S. 2023. Numerical analysis of large masonry structures: bridging meso and macro scales via artificial neural networks. *Computers & Structures,* 283**,** art.number:107042. Available at: https://doi.org/10.1016/j.compstruc.2023.107042.

Krtinić, N., Gams, M. & Marinković, M. 2023. Experimental and numerical investigation of the seismic response of confined masonry walls. In: Papadrakakis, M. & Fragiadakis, M. (Eds.) *ECCOMAS Proceedia COMPDYN 2023 - 9th ECCOMAS Thematic Conference on Computational Methods in Structural Dynamics and Earthquake Engineering*, Athens, Greece, pp.528-543, June 12-14. Available at: https://doi.org/10.7712/120123.10418.20831.

Kulkarni, P., Ravekar, V., Rao, P.R., Waigokar, S. & Hingankar, S. 2022. Recycling of waste HDPE and PP plastic in preparation of plastic brick and its mechanical properties. *Cleaner Materials,* 5, art.number:100113. Available at: https://doi.org/10.1016/j.clema.2022.100113.

Kumar, S. 2022. Challenge 2- Comparing the performance of three types of beams under bending load. *Skill-Lync,* 17 August [online]. Available at: https://skill-lync.com/student-projects/challenge-2-comparing-the-performance-of-three-types-of-beams-under-bending-load-9 [Accessed: 21 April 2024].

Kurian, J.N., Mohan, C.G., Mathew, J., Moolayil, J.T. & Sreekumar, C. 2016. Fabrication of Plastic Brick Manufacturing Machine and Brick Analysis. *IJIRST – International Journal for Innovative Research in Science & Technology,* 2(11), pp.455-462 [online]. Available at: https://ijirst.org/Article.php?manuscript=IJIRSTV2I11139 [Accessed: 21 April 2024].

Lamba, P., Kaur, D.P., Raj, S. & Sorout, J. 2022. Recycling/reuse of plastic waste as construction material for sustainable development: a review. *Environmental Science and Pollution Research,* 29**,** pp.86156-86179. Available at: https://doi.org/10.1007/s11356-021-16980-y.

Lourenço, P.B. 1998. Experimental and numerical issues in the modelling of the mechanical behaviour of masonry. In: Roca, P., Gonzáles, J.L., Onate, E. & Lourenço, P.B. (Eds.) *Structural Analysis of Historical Constructions II. Possibilites of the Numerical and Experimental*, pp.57-91. Barcelona, Spain: International Centre for Numerical Methods in Engineering (CIMNE) [online] Available at: https://repositorium.sdum.uminho.pt/bitstream/1822/66261/1/57.pdf [Accessed: 21 April 2024]. ISBN: 84-89925-26-7.

Lourenço, P.B. 2002. Computations on historic masonry structures. *Progress in Structural Engineering and Materials,* 4(3)**,** pp.301-319. Available at: https://doi.org/10.1002/pse.120.

Lourenço, P.B. & Rots, J.G. 1997. Multisurface Interface Model for Analysis of Masonry Structures. *Journal of Engineering Mechanics,* 123(7)**,** pp.660-668. Available at: https://doi.org/10.1061/(ASCE)0733-9399(1997)123:7(660).

Magomedov, I.A. & Sebaeva, Z.S. 2020. Comparative study of finite element analysis software packages. *Journal of Physics: Conference Series*, 1515, art.number:032073. Available at: https://doi.org/10.1088/1742-6596/1515/3/032073.

Mahmoudi, N. 2014. Effect of volume fiber and crack length on interlaminar fracture properties of glass fiber reinforced polyester composites (GF/PO composites). *Mechanica,* 20(2)**,** pp.153-157. Available at: https://doi.org/10.5755/j01.mech.20.2.6934.

Mahmoudi, N. 2015. Improvement of mechanical and tribological properties of carbon fiber reinforced peek composite filled with carbon nanotubes. *Annales de Chimie - Science des Matériaux*, 39(1-2), pp.1-10.

Mojsilović, N., Simundic, G. & Page, A. 2009. Static-cyclic shear tests on masonry wallettes with a damp-proof course membrane. *IBK Bericht*, 319. Available at: https://doi.org/10.3929/ethz-a-006068632.

Moulai Arbi, Y., Mahmoudi, N. & Djebli, A. 2023. Manufacturing and testing of waste PET reinforced with sand bricks. *Journal of Composite Materials,* 57(16)**,** pp.2513-2526. Available at: https://doi.org/10.1177/00219983231175203.

Nela, B. & Grajçevci, F. 2019. Numerical approach: FEM testing of masonry specimens with different bond configurations of units. In: *Proceedings of Congress on Numerical Methods in Engineering (CMN)*, Guimarães, Portugal, pp.962-978, July 01-03 [online]. Available at: https://www.ehu.eus/documents/13131748/23070166/17.+Thermal+modelling_CMN2019.pdf/b08ec9a0-25ee-96d1-9fe3-0b7bed78b67f?t=1602150875189 [Accessed: 21 April 2024].

-OriginLab. 2020. *OriginPro 2020*. Northampton, MA, USA: OriginLab Corporation.

Pacheco-Torgal, F., Khatib, J., Colangelo, F. & Tuladhar, R. 2018. *Use of Recycled Plastics in Eco-efficient Concrete, 1st Edition.* Woodhead Publishing. ISBN: 9780081027332.

Pandey, B.H. & Meguro, K. 2004. Simulation of brick masonry wall behavior under in-plane lateral loading using applied element method. In: *13th World Conference on Earthquake Engineering*, Vancouver, B.C., Canada, Paper No.

1664, August 1-6 [online]. Available at: https://www.iitk.ac.in/nicee/wcee/article/13_1664.pdf [Accessed: 21 April 2024].

Petracca, M., Pelà, L., Rossi, R., Zaghi, S., Camata, G. & Spacone, E. 2017. Micro-scale continuous and discrete numerical models for nonlinear analysis of masonry shear walls. *Construction and Building Materials,* 149**,** pp.296-314. Available at: https://doi.org/10.1016/j.conbuildmat.2017.05.130.

Ponte, M., Milosevic, J. & Bento, R. 2019. Parametrical study of rubble stone masonry panels through numerical modelling of the in-plane behaviour. *Bulletin of Earthquake Engineering,* 17**,** pp.1553-1574. Available at: https://doi.org/10.1007/s10518-018-0511-9.

Radnić, J., Matešan, D., Harapin, A., Smilović, M. & Grgić, N. 2012. Numerical Model for Static and Dynamic Analysis of Masonry Structures. In: Öchsner, A., da Silva, L. & Altenbach, H. (Eds.) *Mechanics and Properties of Composed Materials and Structures. Advanced Structured Materials,* 31, pp.1-33. Berlin, Heidelberg: Springer. Available at: https://doi.org/10.1007/978-3-642-31497-1_1.

Rafiee, A. & Vinches, M. 2013. Mechanical behaviour of a stone masonry bridge assessed using an implicit discrete element method. *Engineering Structures,* 48**,** pp.739-749. Available at: https://doi.org/10.1016/j.engstruct.2012.11.035.

Rahim, A.B., Noguez, C.C. & Pettit, C. 2024. Experimental Testing of Partially Grouted Masonry Shear Walls with Different Horizontal Reinforcement Types. In: Gupta, R., et al. (Eds.) *Proceedings of the Canadian Society of Civil Engineering Annual Conference CSCE 2022. Lecture Notes in Civil Engineering,* 359, pp.189-207. Cham: Springer. Available at: https://doi.org/10.1007/978-3-031-34027-7_13.

Raijmakers, T.M.J. 1992. *Deformation controlled tests in masonry shear walls: report B-92-1156*. Delft, Netherlands: TNO Bouw.

Ramos Huarachi, D.A., Gonçalves, G., de Francisco, A.C., Canteri, M.H.G. & Piekarski, C.M. 2020. Life cycle assessment of traditional and alternative bricks: A review. *Environmental Impact Assessment Review,* 80**,** art.number:106335. Available at: https://doi.org/10.1016/j.eiar.2019.106335.

Rashid, K., Ul Haq, E., Kamran, M.S., Munir, N., Shahid, A. & Hanif, I. 2019. Experimental and finite element analysis on thermal conductivity of burnt clay bricks reinforced with fibers. *Construction and Building Materials,* 221**,** pp.190-199. Available at: https://doi.org/10.1016/j.conbuildmat.2019.06.055.

Rezapour, M., Ghassemieh, M., Motavalli, M. & Shahverdi, M. 2021. Numerical Modeling of Unreinforced Masonry Walls Strengthened with Fe-Based Shape Memory Alloy Strips. *Materials,* 14(11)**,** art.number:2961. Available at: https://doi.org/10.3390/ma14112961.

Roca, P., Cervera, M., Gariup, G. & Pela', L. 2010. Structural Analysis of Masonry Historical Constructions. Classical and Advanced Approaches. *Archives of Computational Methods in Engineering,* 17**,** pp.299-325. Available at: https://doi.org/10.1007/s11831-010-9046-1.

Sarhosis, V., Garrity, S.W. & Sheng, Y. 2015. Influence of brick–mortar interface on the mechanical behaviour of low bond strength masonry brickwork lintels. *Engineering Structures,* 88**,** pp.1-11. Available at: https://doi.org/10.1016/j.engstruct.2014.12.014.

Sarhosis, V. & Lemos, J.V. 2018. A detailed micro-modelling approach for the structural analysis of masonry assemblages. *Computers & Structures,* 206**,** pp.66-81. Available at: https://doi.org/10.1016/j.compstruc.2018.06.003.

Singhal, A. & Netula, O. 2018. Utilization of plastic waste in manufacturing of plastic sand bricks. *International Journal of Emerging Technologies and Innovative Research*, 5(6), pp.300-303 [online]. Available at: https://www.jetir.org/view?paper=JETIRC006052 [Accessed: 21 April 2024].

Van Rossum, G. 1995. *Python reference manual*. Amsterdam, The Netherlands: Stichting Mathematisch Centrum - CWI [online]. Available at: https://ir.cwi.nl/pub/5008/05008D.pdf [Accessed: 21 April 2024].

Vargas, L., Sandoval, C., Bertolesi, E. & Calderón, S. 2023. Seismic behavior of partially grouted masonry shear walls containing openings: Experimental testing. *Engineering Structures,* 278**,** art.number:115549. Available at: https://doi.org/10.1016/j.engstruct.2022.115549.

Xia, F., Zhao, K., Zhao, J. & Cui, X. 2024. Experimental Study on the Seismic Performance of Brick Walls Strengthened by Small-Spaced Reinforced-Concrete–Masonry Composite Columns. *Buildings,* 14(1)**,** art.number:184. Available at: https://doi.org/10.3390/buildings14010184.

Zhang, W., Kang, S., Liu, X., Lin, B. & Huang, Y. 2023. Experimental study of a composite beam externally bonded with a carbon fiber-reinforced plastic plate. *Journal of Building Engineering,* 71**,** art.number:106522. Available at: https://doi.org/10.1016/j.jobe.2023.106522.

Zhai, C., Wang, X., Kong, J., Li, S. & Xie, L. 2017. Numerical Simulation of Masonry-Infilled RC Frames Using XFEM. *Journal of Structural Engineering,* 143(10). Available at: https://doi.org/10.1061/(ASCE)ST.1943-541X.0001886.

Evaluación del desempeño estructural de muros de mampostería que incorporan ladrillos de plástico reciclado bajo cargas monótonas y cíclicas.

Youcef Moulai Arbi[a], *Noureddine* Mahmoudi[b], *Mohammed* Bentahar[b]

[a] Universidad de Mustapha Stambouli, Laboratorio de Física Cuántica de Materia y Modelamiento Matemático (LPQ3M), Mascara, República Argelina Democrática y Popular, **autor de correspondencia**

[b] Universidad de Saida Dr. Moulay Tahar, Facultad de Tecnología, Departamento de Ingeniería Civil e Hidráulica, Saida, República Argelina Democrática y Popular

CAMPO: ingeniería mecánica, ingeniería civil
TIPO DE ARTÍCULO: artículo científico original

Resumen:

Introducción/objetivo: Este estudio evalúa el desempeño estructural de muros de mampostería hechos de ladrillos de plástico reciclado bajo cargas monótonas y cíclicas. El propósito fue investigar la viabilidad del uso de ladrillos de plástico reciclado como alternativa para la construcción de mampostería, enfocándose en su viabilidad estructural y posibles beneficios ambientales.

Métodos: Se empleó un enfoque de micro modelado simplificado en Abaqus para simular el comportamiento de estas paredes. Los ladrillos de plástico se representaron con elementos sólidos, mientras que las juntas de mortero se modelaron mediante interacciones cohesivas. El modelo numérico fue validado mediante un análisis de sensibilidad de malla y fue sometido a compresión vertical seguida de carga horizontal.

Resultados: Los hallazgos indicaron una reducción de la resistencia en comparación con los materiales de albañilería tradicionales. Sin embargo, el estudio capturó con éxito la respuesta estructural y la evolución del daño de los muros de mampostería bajo las condiciones de carga especificadas. A pesar de la resistencia reducida, la viabilidad estructural de los ladrillos de plástico reciclado se afirmó firmemente y el comportamiento observado bajo condiciones de carga fue particularmente informativo.

Conclusión: La investigación subrayó el potencial de los ladrillos compuestos de plástico para contribuir a las prácticas de construcción sostenible. Los resultados validaron la viabilidad de incorporar ladrillos de plástico en la construcción, destacando sus beneficios ambientales e implicaciones sostenibles. Este estudio avanzó en el campo de los materiales de construcción sostenibles al demostrar la aplicación práctica y los beneficios del uso de ladrillos de plástico reciclado.

Palabras claves: análisis de elementos finitos, ladrillos plásticos, muro de mampostería, cargas en plano, cargas cíclicas en plano.

Оценка структурных характеристик кладки кирпича из переработанного пластика при монотонной и циклической нагрузке

Юсуф Мулаи Арби[а], *Нуредин* Мамуди[б], *Мухаммед* Бентахар[б]

[а] Университет Мустафы Стамбули, лаборатория квантовой физики материи и математического моделирования (LPQ3M), Маскара, Алжирская Народная Демократическая Республика, **корреспондент**

[б] Университет Саиды „Доктор Мулай Тахар“, технологический факультет, кафедра гражданского строительства и гидравлики, Саида, Алжирская Народная Демократическая Республика

РУБРИКА ГРНТИ: 67.11.00 Строительные конструкции
ВИД СТАТЬИ: оригинальная научная статья

Резюме:

Введение/цель: В данном исследовании оцениваются структурные характеристики кирпичных стен из переработанного пластика при монотонной и циклической нагрузке. Целью исследования было изучение возможности использования кирпича из переработанного пластика в качестве альтернативы кирпичной кладке. В статье особое внимание уделялось структурной устойчивости и потенциальным экологическим преимуществам пластикового кирпича.

Методы: Для моделирования поведения кирпичной стены был использован упрощенный подход к микромоделированию в Abaqus. Пластиковые кирпичи были представлены в виде монолитных элементов, в то время как швы между ними были смоделированы с помощью когезионных взаимодействий. Численная модель прошла валидацию с помощью анализа чувствительности сетки и была подвергнута вертикальному сжатию с последующей горизонтальной нагрузкой.

Результаты: Результаты исследования свидетельствуют о снижении прочности по сравнению с традиционными материалами для кладки. Тем не менее в ходе исследования была успешно зафиксирована структурная реакция и эволюция повреждений кирпичных стен при определенных условиях нагрузки. Несмотря на снижение прочности, структурная устойчивость кирпича из переработанного пластика была убедительно подтверждена, а поведение, наблюдаемое в условиях нагрузки, было особенно информативным.

Выводы: В ходе исследования выявлен потенциал пластикового кирпича из композитных материалов для содействия экологичному строительству. Результаты исследования подтвердили целесообразность использования пластикового кирпича в строительстве, подчеркнув его экологические преимущества и устойчивость. Данное исследование вносит большой вклад в область исследований об экологически чистых строительных материалах, демонстрируя практическое применение и преимущества использования кирпича из переработанного пластика.

Ключевые слова: конечно-элементный анализ, пластиковый кирпич, кирпичная кладка, нагрузка в плоскости, циклическая нагрузка в плоскости.

Процењивање понашања структуре зидова од цигли од рециклиране пластике под монотоним и цикличним оптерећењем

Јусуф Мулаи Арби[а], *Нуредин* Мамуди[б], *Мухамад* Бентахар[б]

[а] Универзитет „Мустафа Стамбоули”, Лабораторија за квантну физику материје и математичко моделирање (LPQ3M),
Маскара, Народна Демократска Република Алжир,
аутор за преписку

[б] Универзитет у Саиди „Др Мулаи Тахар”, Технолошки факултет,
Департман за грађевинарство и хидраулику,
Саида, Народна Демократска Република Алжир

ОБЛАСТ: машинство, грађевинарство
КАТЕГОРИЈА (ТИП) ЧЛАНКА: оригинални научни рад

Сажетак:

Увод/циљ: У раду се анализирају перформансе структуре зиданог зида од рециклираних пластичних цигала под монотоним и цикличним оптерећењем. Циљ је био да се испита могућност коришћења цигли од рециклиране пластике као замена за зидану конструкцију, с фокусом на одрживост структуре и потенцијалну корист за животну средину.

Методе:За симулацију понашања оваквих зидова коришћен је поједностављени приступ микромоделовања у Абакусу. Пластичне цигле представљене су помоћу чврстих елемената, док су спојеви од малтера моделовани путем кохезионих интеракција. Нумерички модел је валидиран помоћу анализе осетљивости мреже и подвргнут је вертикалној компресији, а затим хоризонталном оптерећењу.

Резултати: Резултати указују на смањивање чврстоће у односу на традиционалне материјале за зидање.Међутим, одговор структуре био је успешан, као и еволуција оштећења зиданих зидова под одређеним условима оптерећења. Упркос смањеној чврстоћи, структуре од цигала од рециклиране пластике показале су се као изводљиве, а њихово понашање под условима оптерећења као веома добар извор информација.

Закључак: Испитивање је показало да композитне цигле од пластике имају потенцијал да допринесу одрживој градњи. Резултати су потврдили могућност уграђивања пластичних цигли у конструкције, при чему је наглашена корист за животну средину и одрживост. Такође, унапређена је област одрживих грађевинских материјала јер је потврђена практична примена и корист од коришћења цигли од рециклиране пластике.

Кључне речи: анализа коначних елемената, цигле од пластике, зидани зид, оптерећења у равни, циклична оптерећења у равни.

Paper received on: 22.04.2024.
Manuscript corrections submitted on: 25.09.2024.
Paper accepted for publishing on: 26.09.2024.